



The characterization of graphite felt electrode with surface modification for H₂/Br₂ fuel cell



Linsong Zhang^{a,b}, Zhi-Gang Shao^{a,*}, Xunying Wang^{a,b}, Hongmei Yu^a, Sa Liu^{a,b}, Baolian Yi^a

^a Fuel Cell System and Engineering Laboratory, Dalian Institute of Chemical Physics, Chinese Academy of Sciences, 457 Zhongshan Road, Dalian 116023, PR China

^b Graduate School of the Chinese Academy of Sciences, Beijing 100049, PR China

H I G H L I G H T S

- The cell performance is improved by surface modification.
- Thermal oxidation shows better performance than acidic oxidation.
- The maximum power density is improved to 0.69 W cm^{−2} by thermal oxidation.
- Charge transfer resistance decreases for the increase in oxygen-containing groups.

A R T I C L E I N F O

Article history:

Received 28 January 2013

Received in revised form

9 May 2013

Accepted 13 May 2013

Available online 20 May 2013

Keywords:

Hydrogen bromine fuel cell

Graphite felt electrode

Surface modification

Electrochemistry

A B S T R A C T

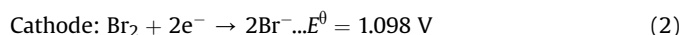
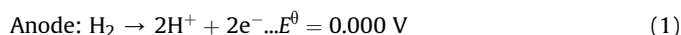
Graphite felt is used as the bromine electrode in H₂/Br₂ fuel cell, which is surface modified by acidic oxidation and thermal oxidation for improving cell performance. The structure, composition, electrochemical properties and performances of the modified electrodes are characterized with X-ray diffraction, scanning electron microscopy, X-ray photoelectron spectroscopy, electrochemistry impedance spectroscopy and single cell polarization curves. The maximum power densities are improved from the original 0.51 to 0.62 and 0.69 W cm^{−2} after acidic oxidized at 80 °C for 8 h and thermal oxidized at 500 °C for 5 h, respectively. The performance improvement may be attributed to the increase in oxygen-containing functional groups and surface area which could increase the electrochemical catalytic activity and thus decrease the charge transfer resistance. However, the ohmic resistance and charge transfer resistance increase after superabundant oxidation, which causes badly deteriorates in cell performance.

© 2013 Elsevier B.V. All rights reserved.

1. Introduction

In recent years, the utilization of renewable energy sources such as solar energy and wind power energy grows quickly. However, the electricity from these renewable sources is not constant and reliable due to the intermittent nature of renewable sources [1,2]. Therefore, large-scale electrical energy storage systems are required to cope with the variable generation of electricity. H₂/Br₂ fuel cell is being considered for affordable grid-scale and intermittent renewable electricity storage due to the high electric-to-electric efficiency (>90% at 108 mA cm^{−2}) because of fast electrochemical reaction kinetics of both the hydrogen and bromine

electrodes [3–6]. The H₂/Br₂ fuel cell consists of a bromine electrode and a hydrogen electrode with a proton-conducting membrane between them. The half-cell reactions in fuel cell are:



The electrochemical reactions for the hydrogen–bromine system are nearly reversible. Consequently, good energy storage efficiencies can be obtained even at high current density operation [5,7]. The electrode catalysts and electrolyte membrane are important components in the cell. Early studies show that the reaction kinetics of both hydrogen and bromine are very fast and nearly reversible on Pt [8,9]. Texas Instruments [10] developed a H₂/Br₂ fuel cell with a porous carbon bromine electrode and the

* Corresponding author. Tel.: +86 411 84379153; fax: +86 411 84379185.
E-mail address: zhgshao@dicp.ac.cn (Z.-G. Shao).

electrolyte of 1 M Br₂ in 6.9 M HBr. They demonstrated a life test for about 10,000 h at current density of 310 mA cm⁻². Recently, Livshits et al. reported that maximum power density of above 1.5 W cm⁻² had been achieved in a H₂/Br₂ fuel cell at 80 °C (0.9 M Br₂ in 1 M HBr), with Pt/C or Pt–Ru/C as bromine catalyst sprayed on Toray paper [11]. The similar bromine electrode was also used by Kreutzer et al. to investigate the regenerative H₂/Br₂ fuel cell [12]. Cho et al. investigated the electrochemical performance of a H₂/Br₂ fuel cell with a positive porous carbon electrode. The high peak power density of 1.4 W cm⁻² and a 91% voltaic efficiency at 0.4 W cm⁻² were achieved at 55 °C with the electrolyte solution of 0.9 M Br₂ in 1 M HBr [13].

Porous carbonaceous materials with high surface area have been extensively used as electrodes in the redox flow battery [14]. In particular, carbon felt or graphite felt, with good electronic conductivity, is an appropriate material to provide abundant reaction sites. However, due to its hydrophobic surface nature and poor kinetics of redox reaction, its wettability and electrochemical activity needs to be improved to generate higher energy efficiency [15]. Consequently, a great deal of effort went into enhancing the electrochemical properties for use in all-vanadium redox flow battery (VRFB) [14,16–20]. However, the characterization of surface modified graphite felt electrode in H₂/Br₂ fuel cell and the correlation between surface nature and electrochemical performance have still not been widely investigated.

In this work, graphite felt was used as the bromine electrode and two surface modifications such as acidic oxidation and thermal oxidation were adopted to improve the cell performance. The modified electrodes were characterized by X-ray diffraction (XRD), scanning electron microscopy (SEM) and X-ray photoelectron spectroscopy (XPS). Their performances were investigated in the H₂/Br₂ fuel cell.

2. Experimental

2.1. Materials

The porous graphite felt made of polyacrylonitrile-base carbon fibers, with high mechanical strength, good electronic conductivity and large specific surface area, was used as bromine electrode. The graphite felt with a thickness of 3 mm was purchased from Hunan Jiuhua Carbon Hi-Tech Co., Ltd., China. H₂SO₄ (98 wt%) and HNO₃ (68 wt%) were purchased from Tianjin Kermel Chemical Reagent Co. Ltd. China.

2.2. Acid oxidation

The graphite felt electrode with the size of 2.0 × 2.0 cm was oxidized in mixed acids (V_{H₂SO₄}/V_{HNO₃} = 3/1). Prior to oxidation, the graphite felt electrodes were sonicated in anhydrous ethanol for 30 min in order to remove impurities, followed by rinsing with deionized water for 30 min and drying in oven at 100 °C for 5 h. This purified graphite felt electrode was denoted as GF. The GF electrodes were oxidized in a sealed 100 mL Teflon-lined flask containing 40 mL mixed acid solution at 80 °C for different durations. The oxidized samples were first washed with deionized water, and then sonicated in the deionized water for 30 min. This procedure was repeated several times until the pH of the rinsed water became neutral. Finally, they were dried in oven at 100 °C for 5 h.

2.3. Mild oxidation

The purified GF electrodes were heated to the desired oxidation temperature in a ceramic tube furnace at a heating rate of 3 °C min⁻¹. The heating temperatures were varied from 400 to

550 °C and the duration was varied from 2 h to 10 h under air atmosphere. Finally, the furnace was cooled down to room temperature.

2.4. Sample physical characterizations

The GF electrodes before and after oxidation were employed to evaluate their physical characterization. X-ray diffraction (XRD) patterns were performed by a PANalytical diffractometer (X'Pert PRO) with a Cu Kα radiation source (λ = 1.54056 Å) to characterize the crystalline structure. The surface morphology of samples was characterized with a scanning electron microscopy (SEM) (JEOL, JSM-6360LV, Japan) at an acceleration voltage of 20 kV. X-ray photoelectron spectroscopy (XPS) spectra were obtained by employing ESCALAB250Xi (Thermo Fisher Scientific, USA) surface analysis system. XPS spectra were analyzed using Spectrum software (XPSPEAK).

2.5. Performance of hydrogen bromine fuel cell

The performance of hydrogen bromine fuel cell was evaluated in a single cell at 30 °C. The cell consisted of two graphite end-plates, a Teflon gasket (2 mm), a bromine electrode, an electrolyte membrane and a hydrogen electrode. GF electrodes before and after oxidation were employed as the bromine electrodes (4 cm²). Gas diffusion electrode with 0.6 mg cm⁻² Pt/C catalyst (70 wt%, Johnson Matthey) was used as hydrogen electrode. The hydrogen electrode was attached to the electrolyte membrane Nafion212 by hot pressing at 140 °C and 1 MPa. Bromine electrode and Nafion212 with hydrogen electrode were positioned between two graphite plates, in which parallel flow fields were engraved. Teflon gasket (2 mm) was applied to seal the bromine electrode. 0.6 mol L⁻¹ Br₂ in 1 mol L⁻¹ HBr (0.5 L) was circulated over the cathode, and dry hydrogen with pressure of 0.05 MPa was fed to the anode. Electrochemistry impedance spectroscopy (EIS) was carried out at open circuit voltage (OCV) with PARSTAT 2273 (EG&G Instruments). The frequency varied from 10 kHz to 100 mHz and 10 mV amplitude of sinusoidal potential perturbation was employed. The obtained impedance data were simulated with ZSimpWin software.

3. Results and discussion

3.1. XRD and SEM characterization

The graphite felt electrodes before and after acidic oxidation and thermal oxidation were characterized by XRD and the results are shown in Figs. 1 and 2. It is clear that the most significant diffraction peak is the (002) plane located at 26.4° for all samples. Two weak diffraction peaks at about 43.5° and 54.3° correspond to (100) and (004) planes, respectively [17,21]. By comparing the XRD patterns of GF electrodes, it can be found that the XRD patterns show a dramatic decrease in diffraction intensity after oxidation. And the diffraction intensity decreases with the increasing oxidation temperature and duration. These results demonstrate that more structure defects are introduced by oxidation [17]. This can be confirmed by the observation with SEM in Figs. 4 and 5. The weakened diffraction peaks are attributed to the partial disordering of in-plane reflection plane cause by defects.

To investigate the surface morphology changes introduced by oxidation, scanning electron microscopy (SEM) was conducted and the results are shown in Fig. 3. The surface of GF is smooth and no visible changes are observed after acidic oxidation. May be only micro changes were introduced at the surface and physical structure remained intact during acidic oxidation. Figs. 4 and 5 show the SEM images for the effect of thermal oxidation. Obvious

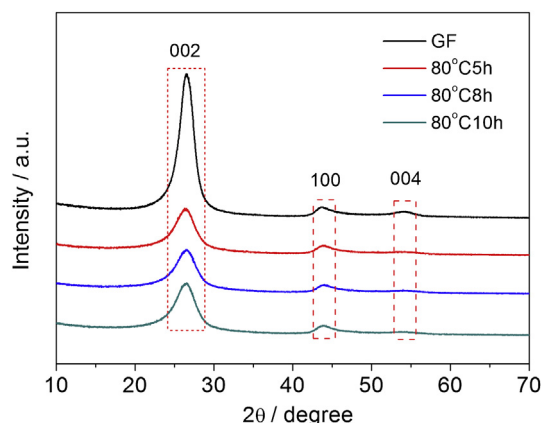


Fig. 1. XRD patterns of the graphite felt electrodes before and after acidic oxidation.

morphology changes can be induced by thermal oxidation. The surface roughness was enhanced with the increase in oxidation temperature and oxidation time. It can be seen that few small cavities appeared on the surface after thermal oxidized at 500 °C for 2 h, a fair amount of cavities for 5 h. The small cavities will increase the surface area of graphite felt [14]. Moreover, the samples were badly corroded and the fibers became thinner after being thermal oxidized at 550 °C for 5 h or 500 °C for 10 h. The surface complex was decomposed by the evolution of carbon dioxide at elevated temperature and prolonged oxidation time, which leads to a dramatic increase in the weight loss of graphite felt [16]. Accordingly, it

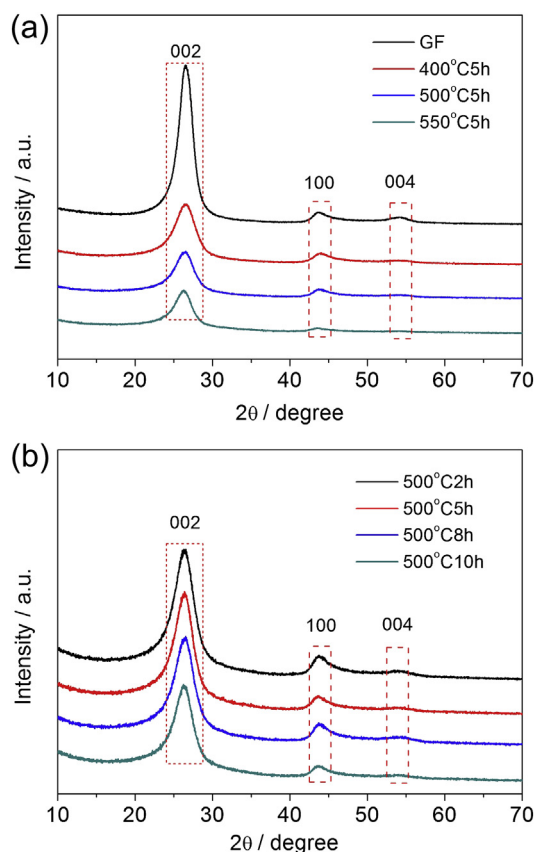


Fig. 2. XRD patterns of the graphite felt electrodes before and after thermal oxidation: (a) the effect of oxidation temperature, (b) the effect of oxidation time.

is reasonable to infer that the mechanical strength of graphite felt was deteriorated. The thermal oxidation temperature should not be higher than 500 °C or last more than 5 h to avoid the decline in mechanical strength of material.

3.2. EIS analysis

Electrochemical impedance spectroscopy (EIS) is a very useful tool to investigate the electrode reaction process, especially the charge transfer resistance at the electrolyte/electrode interface. An analysis of the electrochemical impedance was carried out at OCV and 30 °C. A comparison of Nyquist plots is reported in Fig. 6. It obviously indicates the existence of inductance, L , at high frequencies. The inductance may be the consequence of the porous nature of graphite felt or the electrical lead of equipment [22]. The impedance parameters are obtained from fitting the experimental data and listed in Table 1. The equivalent circuit can be described as $LR_Q(R_1Q_1)(R_{ct}Q_{dl})$. L is the inductance and R_Q represents the total ohmic resistance of the single cell. R_{ct} is a measure of charge transfer resistance at the electrolyte/electrode interface. Q_{dl} is the constant phase elements and represents the capacitive elements. Generally, R_1Q_1 circuit is attributed to the diffusion phenomena [17,23,24]. It can be seen in Table 1, the cell resistance drops initially after acid treatment, followed by a slight increase after prolonged treatment. The results are consistent with previous reports by Sun and Skyllas-Kazacos [18]. The sample treated at 80 °C for 10 h possesses bigger resistances than the other acid treated samples. It may be attributed to the increase of C=O group generated from further oxidation of –OH and C=O further oxidized into carbon dioxide [17].

The fitting results show that the R_Q before and after acidic oxidation are around 0.20 $\Omega \text{ cm}^2$. However, the R_Q values increase significantly when the temperature is higher than 500 °C or the time is longer than 5 h for thermal oxidation samples. The results from this study are consistent with previous reports [16]. The increase in ohmic resistance will deteriorate the cell performance. As shown in Table 1, the R_{ct} and R_1 values decrease obviously after oxidation. The electrodes acidic oxidized at 80 °C for 8 h, thermal oxidized at 400 °C and 500 °C for 5 h have smaller R_{ct} values. Additionally, the charge transfer resistance R_{ct} of thermal oxidation is smaller than that of acidic oxidation, which further suggests that the thermal oxidized electrodes yield higher electrochemical catalytic activity [21]. These results are certainly consistent with the fuel cell performance in Figs. 7 and 8.

3.3. The hydrogen/bromine fuel cell performance

A hydrogen/bromine single fuel cell was used to examine the performance of the electrodes before and after oxidation. Fig. 7 shows the effect of acidic oxidation on the cell performance, in which it is clear that the electrode oxidized at 80 °C for 8 h yields the best performance in all regions of the polarization curve. The maximum power densities are 0.51 W cm^{-2} and 0.62 W cm^{-2} for GF electrode and modified electrode, respectively. There is dramatic performance drop in the low current density region (i.e. less than 0.2 A cm^{-2}) for the case of the GF electrode, indicating huge activation loss (i.e. kinetic loss) due to the low kinetics of bromine on GF. However, the performance drop is alleviated for the modified electrodes. It means that the modified electrodes possess a faster rate of bromine reduction [24,25]. And the result is in accordance with the EIS test results in Fig. 6(a). Accordingly, the improvement in performance is attributed to the increase in electrochemical catalytic activity for the acidic oxidation.

The effect of thermal oxidation on the cell performances is shown in Fig. 8. The performances first increase and then decrease

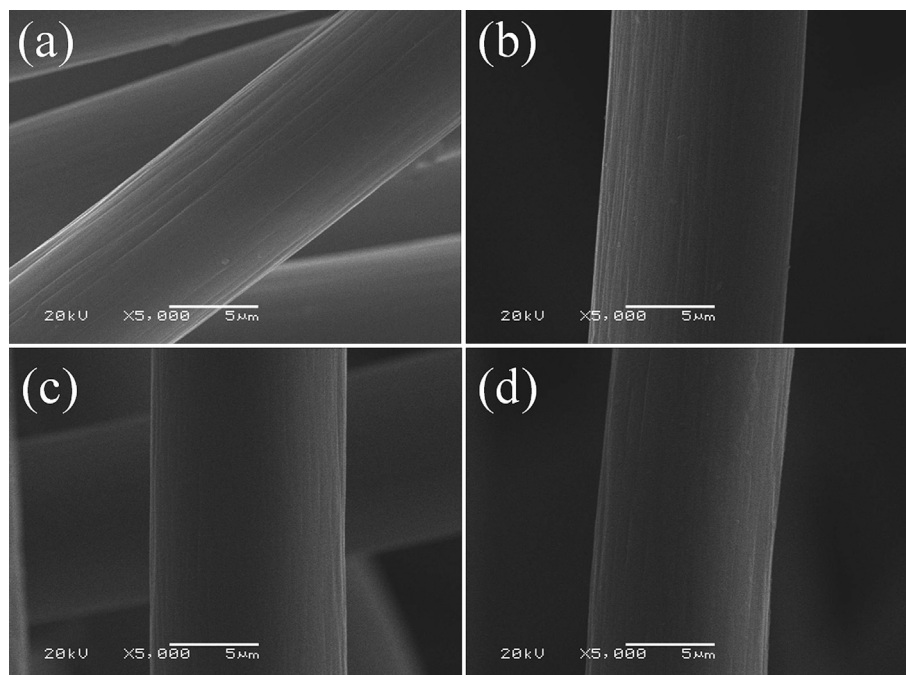


Fig. 3. SEM images of the graphite felt electrodes before and after acidic oxidation: (a) GF, (b) 80 °C for 5 h, (c) 80 °C for 8 h and (d) 80 °C for 10 h.

with increasing oxidation temperature and oxidation time. The electrodes oxidized at 400 °C and 500 °C for 5 h are better than the others and the maximum power densities are 0.68 and 0.69 W cm⁻², respectively. Compare to GF electrode, the maximum power densities are enhanced by 35% and 22% for thermal and acidic oxidation, respectively. This indicates that thermal oxidation is more effective than acid oxidation to improve electrochemical catalytic activity. As shown in Fig. 8(a), there is significant enhancement at the low current density region (i.e. kinetic-

dominant region) for the electrodes after proper thermal oxidation, thus indicating the reaction kinetics is improved dramatically by thermal oxidation. Although the low and intermediate current density performances are comparable, the high current density region (i.e. bigger than 1.2 A cm⁻²) is significantly affected by mass-transfer losses for the electrode oxidized at 400 °C due to its low hydrophilicity. Furthermore, the oxidation temperature and duration of thermal oxidation are very important factors that influence the cell performance. As shown in Fig. 8, there are noticeable

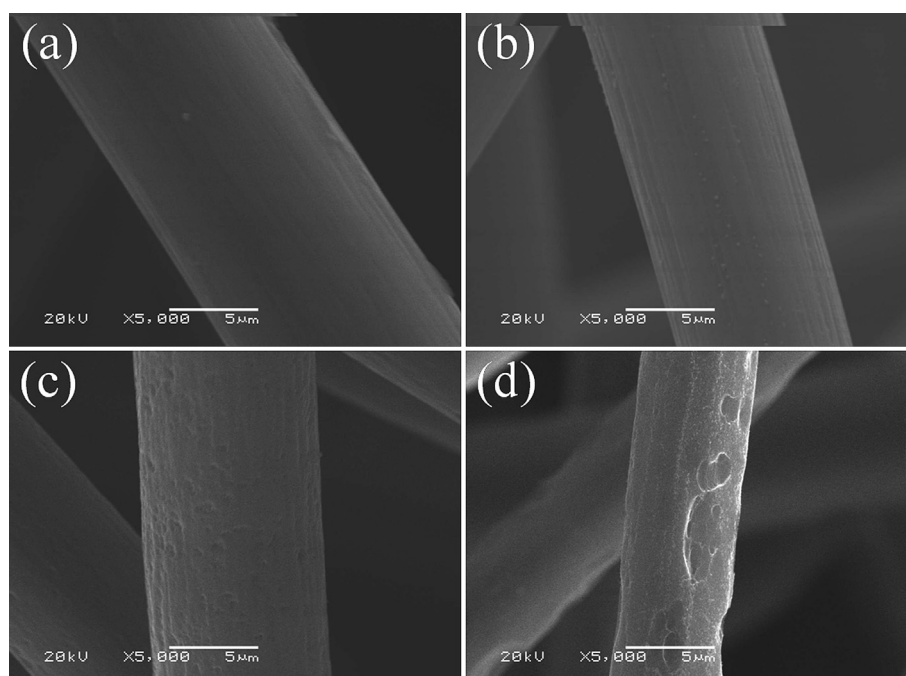


Fig. 4. SEM images of the graphite felt electrodes before and after thermal oxidation: (a) GF, (b) 400 °C for 5 h, (c) 500 °C for 5 h and (d) 550 °C for 5 h.

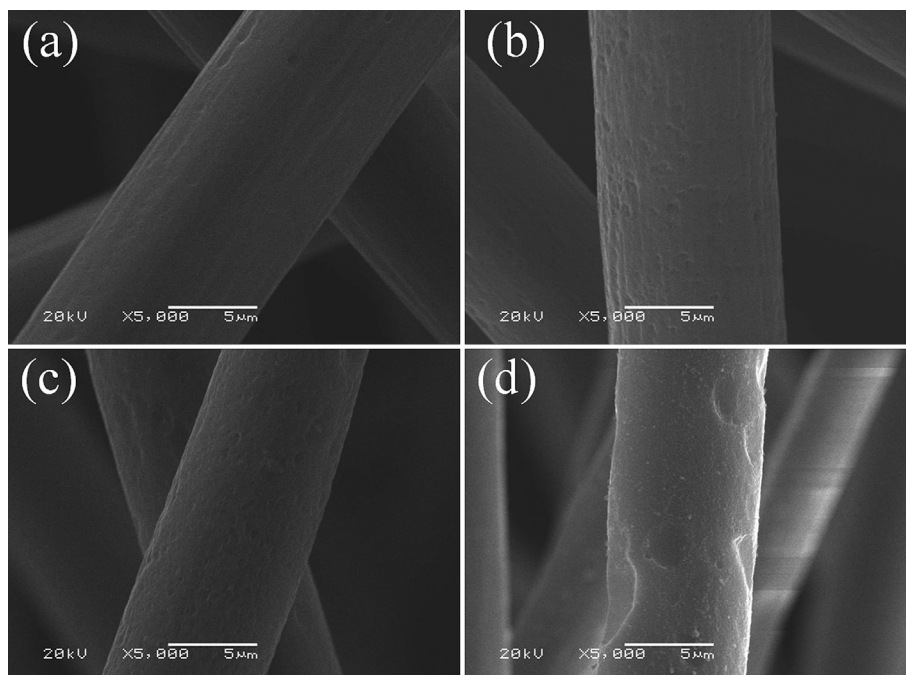


Fig. 5. SEM images of the graphite felt electrodes after thermal oxidation: (a) 500 °C for 2 h, (b) 500 °C for 5 h, (c) 500 °C for 8 h and (d) 500 °C for 10 h.

deteriorations in the cell performance when the oxidation temperature is higher than 500 °C and oxidation time is longer than 5 h. The cell performance is fully controlled by ohmic resistance. The ohmic resistances obtained from fitting the EIS data are given in Table 1. From Table 1, the electrode oxidized at 550 °C for 5 h possesses the biggest ohmic resistance $1.15 \Omega \text{ cm}^2$, which is about five times bigger than that of GF electrode ($0.21 \Omega \text{ cm}^2$). Moreover, the ohmic resistance of electrode oxidized at 500 °C for 10 h ($0.76 \Omega \text{ cm}^2$) and 8 h ($0.70 \Omega \text{ cm}^2$) are also much higher than that of GF electrode. The higher ohmic resistance leads to a lower cell performance than the rest.

Base on the above-mentioned analyses, cell performance depends on the oxidation temperature and oxidation duration. It was reported that 400 °C was the optimum temperature for maximum fixation of oxygen and the surface complex was decomposed by the evolution of carbon dioxide at 500 °C [16]. It can be seen from the surface morphology in Fig. 5 that the burn off of graphite felt increases with prolonged oxidation time at 500 °C. Notably, when oxidation temperature is higher than 500 °C, such as 530 °C and 550 °C, the decomposition kinetics of surface complex is improved. And a sharp increase in resistance is obtained due to carbon oxide formed rapidly in air at high temperature with prolonged time [26]. Therefore, superabundant oxidation will damage the structure and increase the ohmic resistance. According to the comparison between the two surface modifications, the thermal oxidized electrodes possess higher electrochemical catalytic activity than acidic oxidized electrodes.

3.4. XPS analysis

In order to analyze the high performance of the modified electrode, it is necessary to conduct further study to find out the types of functional groups mainly responsible for the enhancement of the electrode activity. XPS is a suitable technique particularly for monitoring the functional groups in the surface region. The electrodes which have the best performance of the two surface modifications, acidic oxidation at 80 °C for 8 h and thermal oxidation at

500 °C for 5 h were investigated. Wide scan spectra in the binding energy range 0–1000 eV were obtained to identify the surface elements and carry out a quantitative analysis. Fig. 9 shows the XPS survey spectra and O1s spectra of different samples. As shown in Fig. 9, the intensity of the O1s peak at the binding energy of 532 eV increases significantly after oxidation, which indicates that the O content increases. Table 2 lists the contents of surface elements and oxygen-containing groups which can be obtained from Fig. 9. The results show noticeable increase in O contents after the acidic and thermal oxidation, the contents of O are 13.8 At% and 11.8 At%, respectively, in contrast to the case of GF 6.5 At%.

For quantitative analysis of various oxygen-containing functional groups, the O1s XPS spectra were fitted by three peaks. According to the literature, the component around 531.8 eV was attributed to carboxylic or carbonyl groups [27], the peak at 532.2–532.8 eV was attributed to oxygen of phenol and alcohol [17,27], and the peak around 535 eV was assigned to the absorbed water and some chemical absorbed oxygen [14,17]. The fitting results are listed in Table 2. It shows an increase in the contents of all oxygen-containing groups after oxidation. The content of C=O increases to 5.1 At% and 2.9 At%, and –OH to 6.5 At% and 6.3 At% after acidic oxidation and thermal oxidation, respectively. The contents of –OH groups are approximate. It shows that thermal oxidation benefits the formation of –OH groups. The –OH groups mainly come from the breakage of C=C bonds on the fragments under strong oxidation and the C=O groups result from the further oxidation of –OH groups [28]. With further oxidation, the C=O groups are oxidized into carbon dioxide, which results in many cavities on the surface. From Figs. 4 and 5, it can be seen that rough surface is obtained by thermal oxidation. It is noteworthy that a larger surface area would be favorable to enhance the reaction of bromine for more reaction sites and function groups are provided.

Since the reactant bromine is dissolved in water solution, the hydrophilicity of graphite felt is very important for the bromine electrode reaction. The increase of hydroxyl and carboxyl groups on the fiber surface improves its polarity, which can enhance the hydrophilicity and water adsorption ability of bromine electrode [14].

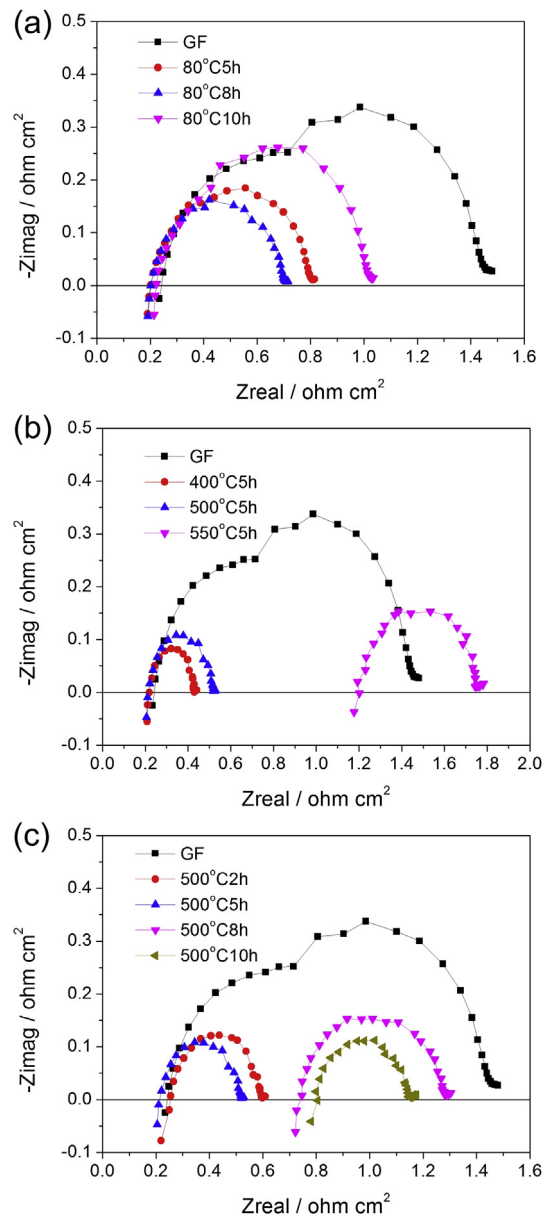


Fig. 6. The Nyquist diagrams of the hydrogen bromine fuel cell at 30 °C using different graphite felt electrodes: (a) acidic treatment, (b) thermal oxidation at different temperature, (c) thermal oxidation for different time.

It can be confirmed by the increased water content shown in Table 2. As a result more electrolytes can be absorbed on the modified electrodes. The improved electrochemical activity can be ascribed to the plenty of oxygen functional groups on the surface, which behave as

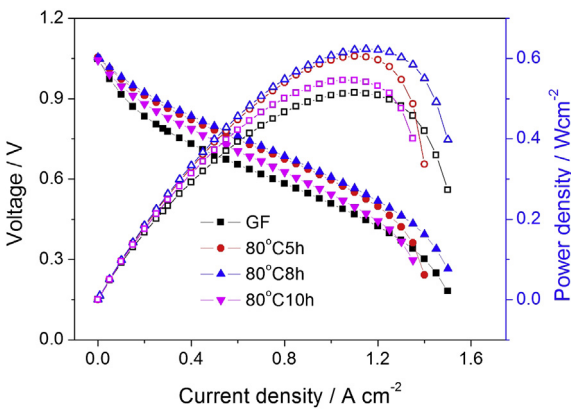


Fig. 7. Effect of acidic oxidation on cell performance.

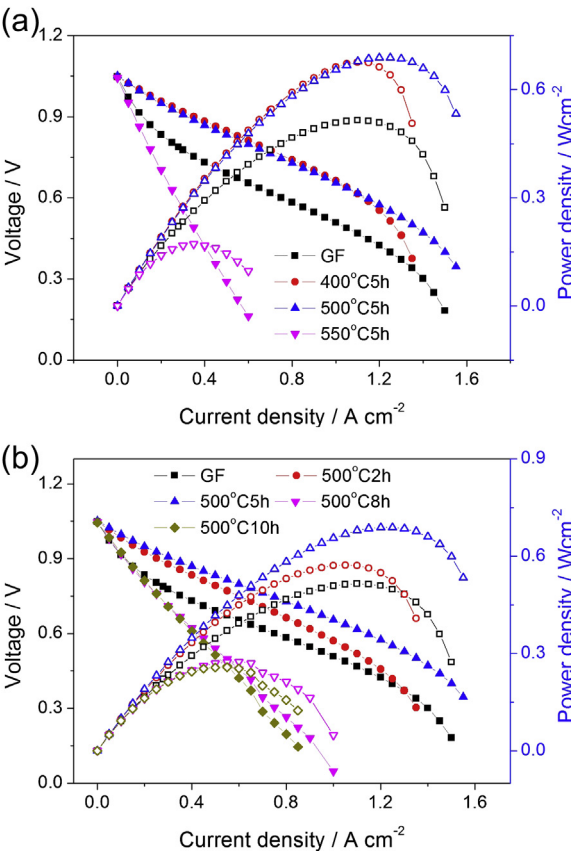


Fig. 8. Effect of thermal oxidation on cell performance: (a) different temperature, (b) different time.

Table 1
Impedance parameters obtained from fitting the experimental data to the $LR_0(R_1Q_1)(R_{ct}Q_{ct})$ circuit for GF electrodes before and after oxidation.

Samples	GF	Acidic oxidation			Thermal oxidation					
		80 °C			400 °C		500 °C		550 °C	500 °C
		5 h	8 h	10 h	5 h	5 h	5 h	2 h		
R_0 (Ω cm ²)	0.21	0.18	0.18	0.20	0.20	0.19	1.15	0.23	0.70	0.76
R_{ct} (Ω cm ²)	0.82	0.53	0.38	0.62	0.23	0.33	0.50	0.37	0.52	0.40
R_1 (Ω cm ²)	0.46	0.11	0.16	0.18	0.06	0.01	0.13	0.01	0.08	0.02

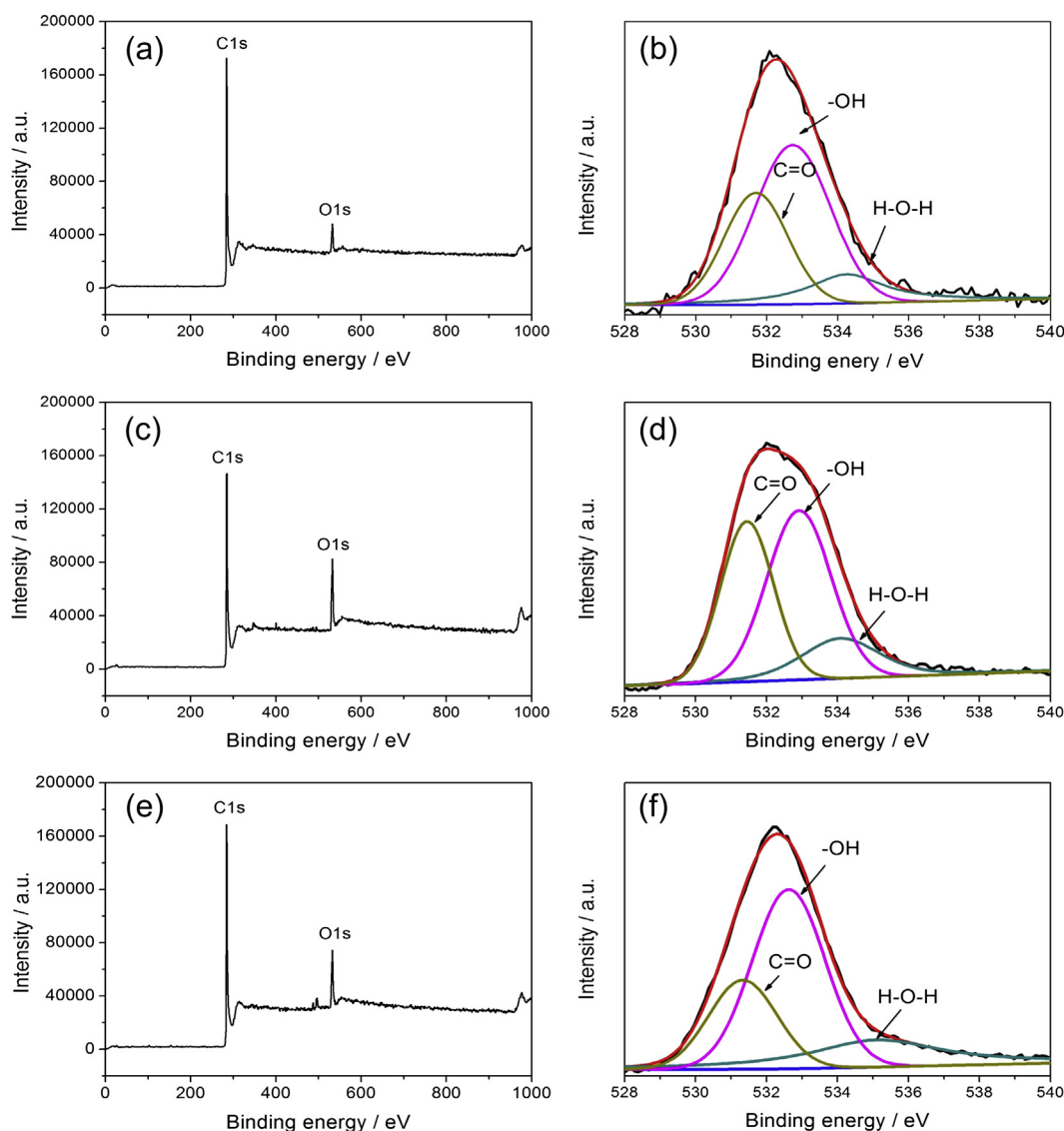


Fig. 9. XPS general spectra and curve-fit of O1s spectra from GF (a and b), acidic oxidation at 80 °C for 8 h (c and d), thermal oxidation at 500 °C for 5 h (e and f).

active sites and catalyze the reduction processes [2]. Besides oxygen functional groups, the surface area of electrode is another important factor for electrochemical activity. Based on the structural analyses, it is noteworthy that the thermal oxidized graphite felt has a larger surface area. A large surface area would be favorable for enhancing the reduction reactions because it could provide more reaction sites and functional groups. That may be the reason why thermal oxidation with lower oxygen content is more effective in enhancing the performance than acidic oxidation. Researches

show that the $-OH$ groups are more favorable to improve the electrochemical activity in all-vanadium redox flow battery [17,29–31]. However, the reactants of the bromine electrode are anions Br_3^- in the H_2/Br_2 fuel cell; on the contrary, the reactants of the vanadium electrode are cations VO_2^+/VO^{2+} in the VRFB. Therefore, the functional groups mainly responsible for the enhancement of the electrode activity and the catalytic mechanism of oxygen functional groups should be investigated to further improve the electrochemical activity.

Table 2

The contents of surface elements and oxygen-containing groups on the surface of GF electrodes before and after oxidation: acidic oxidation 80 °C 8 h, thermal oxidation 500 °C 5 h.

Sample	C content $x_{At}\%$	O content $x_{At}\%$	C=O content $x_{At}\%$	$-OH$ content $x_{At}\%$	H–O–H content $x_{At}\%$
GF	93.5	6.5	2.0	3.5	1.0
Acidic oxidation	86.2	13.8	5.1	6.5	2.2
Thermal oxidation	88.2	11.8	2.9	6.3	2.6

4. Conclusions

Surface modification is an effective way to improve the electrochemical catalytic activity for graphite felt which is used as bromine electrode in the H_2/Br_2 fuel cell. When the electrodes are acidic oxidized at 80 °C for 8 h and thermal oxidized at 500 °C for 5 h, the cell exhibited improved maximum power densities from 0.51 to 0.62 and 0.69 $W\ cm^{-2}$, respectively. However, the ohmic resistance and charge transfer resistance increase after superabundant oxidation, which causes significant deteriorates in the cell performance. The enhanced activities of the modified

electrodes may be attributed to the increase in oxygen-containing functional groups on the surface of the modified electrodes. The thermal oxidation not only increases the oxygen content but also the surface area. Accordingly, the thermal oxidized electrodes show better performance than the acidic oxidized electrodes. The increasing electrochemical activity suggests that the oxygen-containing functional groups play an important role in catalyzing bromine reduction reaction. Moreover, the types of functional groups on the surface are critical to determine the kinetics of the reaction. More detailed work on the relation between the electrochemical activities and functional groups and the mechanism of bromine redox reaction on the GF electrodes is highly required.

Acknowledgements

We thank the National High Technology Research and Development Program of China (863 Program, 2011AA050701 and 2012AA052002) and the National Natural Science Foundations of China (Nos. 20936008 and 21076208) for financial support.

References

- [1] Z. Yang, J. Zhang, M.C.W. Kintner-Meyer, X. Lu, D. Choi, J.P. Lemmon, J. Liu, *Chem. Rev.* 111 (2011) 3577–3613.
- [2] W. Wang, Q. Luo, B. Li, X. Wei, L. Li, Z. Yang, *Adv. Funct. Mater.* 23 (2013) 970–986.
- [3] R.F. Savinell, S.D. Fritts, *J. Power Sources* 22 (1988) 423–440.
- [4] R.S. Yeo, D.T. Chin, *J. Electrochem. Soc.* 127 (1980) 549–555.
- [5] J.A. Kosek, A.B. Laconti, *J. Power Sources* 22 (1988) 293–300.
- [6] F. Mitlitsky, B. Myers, A.H. Weisberg, *Energ. Fuel* 12 (1998) 56–71.
- [7] S.D. Fritts, R.F. Savinell, *J. Power Sources* 28 (1989) 301–315.
- [8] I. Rubinstein, *J. Phys. Chem.* 85 (1981) 1899–1906.
- [9] G.G. Barna, S.N. Frank, T.H. Teherani, *J. Electrochem. Soc.* 129 (1982) 2464–2468.
- [10] G.G. Barna, S.N. Frank, T.H. Teherani, L.D. Weedon, *J. Electrochem. Soc.* 131 (1984) 1973–1980.
- [11] V. Livshits, A. Ulus, E. Peled, *Electrochem. Commun.* 8 (2006) 1358–1362.
- [12] H. Kreutzer, V. Yarlagadda, T. Van Nguyen, *J. Electrochem. Soc.* 159 (2012) F331–F337.
- [13] K.T. Cho, P. Ridgway, A.Z. Weber, S. Haussener, V. Battaglia, V. Srinivasan, *J. Electrochem. Soc.* 159 (2012) A1806–A1815.
- [14] K.J. Kim, Y.-J. Kim, J.-H. Kim, M.-S. Park, *Mater. Chem. Phys.* 131 (2011) 547–553.
- [15] W. Li, J. Liu, C. Yan, *Carbon* 49 (2011) 3463–3470.
- [16] B. Sun, M. Skyllas-Kazacos, *Electrochim. Acta* 37 (1992) 1253–1260.
- [17] L. Yue, W. Li, F. Sun, L. Zhao, L. Xing, *Carbon* 48 (2010) 3079–3090.
- [18] B. Sun, M. Skyllas-Kazacos, *Electrochim. Acta* 37 (1992) 2459–2465.
- [19] X.-g. Li, K.-l. Huang, S.-q. Liu, N. Tan, L.-q. Chen, *Trans. Nonferr. Metal. Soc.* 17 (2007) 195–199.
- [20] Z. González, A. Sánchez, C. Blanco, M. Granda, R. Menéndez, R. Santamaría, *Electrochem. Commun.* 13 (2011) 1379–1382.
- [21] W. Li, J. Liu, C. Yan, *Electrochim. Acta* 56 (2011) 5290–5294.
- [22] Z.-G. Ye, H.-M. Meng, D.-B. Sun, *J. Electroanal. Chem.* 621 (2008) 49–54.
- [23] J. Cheng, H. Zhang, G. Chen, Y. Zhang, *Electrochim. Acta* 54 (2009) 6250–6256.
- [24] X. Yuan, H. Wang, J. Colin Sun, J. Zhang, *Int. J. Hydrogen Energy* 32 (2007) 4365–4380.
- [25] H. Su, B.J. Bladergroen, V. Linkov, S. Pasupathi, S. Ji, *Int. J. Hydrogen Energy* 36 (2011) 15081–15088.
- [26] H.Q. Zhu, Y.M. Zhang, L. Yue, W.S. Li, G.L. Li, D. Shu, H.Y. Chen, *J. Power Sources* 184 (2008) 637–640.
- [27] Y. Lu, J. Chen, H. Cui, H. Zhou, *Compos. Sci. Technol.* 68 (2008) 3278–3284.
- [28] D.B. Mawhinney, V. Naumenko, A. Kuznetsova, J.T. Yates Jr., J. Liu, R.E. Smalley, *Chem. Phys. Lett.* 324 (2000) 213–216.
- [29] D. Yang, G. Guo, J. Hu, C. Wang, D. Jiang, *J. Mater. Chem.* 18 (2008) 350–354.
- [30] Z. Kang, E. Wang, B. Mao, Z. Su, L. Gao, L. Niu, H. Shan, L. Xu, *Appl. Catal. A: Gen.* 299 (2006) 212–217.
- [31] R. Tian, X. Wang, M. Li, H. Hu, R. Chen, F. Liu, H. Zheng, L. Wan, *Appl. Surf. Sci.* 255 (2008) 3294–3299.